Pergamon

Int. J. Heat Mass Transfer. Vol. 38, No. 12, pp. 2209–2224, 1995

0017-9310/95 $9.50+0.00

0017-9310(94)00343-2

Transient pool boiling from downward-facing curved surfaces

MOHAMED S. EL-GENK and ALEXANDER G. GLEBOV

Institute for Space and Nuclear Power Studies and Department of Chemical and Nuclear Engineering, University of New Mexico, Albuquerque, NM 87131, U.S.A.

(*Received* 14 *March* 1994 *and in final form* 26 *October* 1994)

Abstract—Quenching experiments were performed to investigate the effects of wall thickness on pool boiling from downward-facing curved surfaces in water. Experiments employed three copper sections of the same diameter (50.8 mm) and surface radius (148 mm), but of different thicknesses (12.8, 20 and 30 mm). Local and average pool boiling curves were obtained at saturation and 5, 10 and 14 K subcooling. The maximum and minimum film boiling heat fluxes, which increased with increased subcooling, were independent of wall thickness >19 mm and Biot number >0.8 and 0.008, respectively, indicating that boiling curves for the 20 and 30 mm thick sections were representative of quasi steady-state, but not those for the 12.8 mm thick section. When compared to that of a flat surface section of the same material and dimensions, the average pool boiling curve for the 12.8 mm thick section showed significant increases in the maximum heat flux (from 0.21 to 0.41 MW m^{-2}) and the minimum film boiling heat flux (from 2 to 13 kW m^{-2}) and about 11.5 and 60 K increase in the corresponding wall superheats, respectively.

INTRODUCTION

Several studies reported pool boiling from inclined and downward-facing flat surfaces in saturated R-11, helium, nitrogen, isopropyl alcohol and water [1–12] using steady-state heating. Beduz *et al.* [2], Githinji and Sabersky [4] and Nishikawa *et al.* [9] have shown that the surface average nucleate boiling heat flux increases; the maximum heat flux, however, decreases as surface inclination angle, θ, decreases. In these studies, the inclination angle, θ, was varied from 5° to 180° (upward-facing); little data was reported for the downward-facing position ($\theta = 0°$). Recently, Guo and El-Genk [13, 14] and El-Genk and Guo [15, 16] performed quenching experiments using a flat surface copper test section, 50.8 mm in diameter and 12.8 mm thick, in saturated and subcooled water at θ of 0, 5, 10, 15, 30, 45 and 90° (vertical). Their surface average saturation nucleate boiling heat fluxes at low wall superheat agreed qualitatively with those of Nishikawa *et al.* [9] and Beduz *et al.* [2], and for the maximum heat flux with those of Vishnev *et al.* [12] and Beduz *et al.* [2] for saturation boiling.

The results of Guo and El-Genk as well as those of other investigators [1–16] are, however, not applicable to pool boiling from downward-facing curved surfaces, for which, to the best of the authors knowledge, there is very little experimental data available [17, 18]. Pool boiling on the inside and the outside of downward-facing curved surfaces is of interest to workers in many fields. A few examples include handling of hazardous and liquid chemicals during fire in chemical industry, thermal management of cryogenic liquids in ground storage in aerospace industry, cooling of electric cables with pool boiling of liquid helium in superconductivity research and telecommunication industry, and nuclear reactor safety.

In nuclear reactor safety, a concern is the coolability of the bottom heads of Advanced Light Water Reactor (ALWR) pressure vessels, following a core meltdown accident [19–21]. In such an accident, molten fuel, cladding and control material will flow downward under the influence of gravity, and may eventually collect in the bottom head of the reactor vessel. Once in the bottom head, the molten core materials will heat the structure and can eventually melt through the wall, unless adequate cooling can be provided. In the Three Mile Island unit 2 (TMI-2) accident, partial melting of the reactor core and significant oxidation and release of fission products from the fuel occurred. It was estimated that approximately 45% of the core had melted and 20% (~19 metric tons) of the molten core materials relocated into the bottom head of the reactor vessel. Examination of the bottom head samples revealed the presence of a localized hot spot covering an elliptical region measuring 1.0 m × 0.8 m, where the temperature could have reached ~1370 K for about 30 mins. The inside surface temperature of the vessel lower head outside the hot spot region remained below ~900 K. Although no failure of the vessel occurred, such a hot spot could shorten the time to vessel failure due to creep rupture. Therefore, it is important to investigate passive cooling strategies of the bottom head to prevent vessel failure by creep rupture. One accident management strategy under consideration for ALWRs is to passively cool the external surface of the vessel bottom head by pool boiling of water in the underlying cavity. It is hoped that cooling the bottom head by pool boiling will

NOMENCLATURE

a_0, a_1, a_2 coefficients, equation (5)
Bi surface average Biot number, $(\bar{q} \cdot H/((\overline{\Delta T_{sat}} + \Delta T_{sub})\overline{k_{cu}}))$
C_p specific heat [kJ kg^{-1} K^{-1}]
H test section thickness [m]
k thermal conductivity [W m^{-1} K^{-1}]
MHF maximum heat flux
q surface heat flux [MW m^{-2}]
r radial coordinate
R radius [m]
t time [s]
T temperature [K]
z axial coordinate.

Greek symbols
δ coefficient, equation (4)
ΔT_{sat} local wall superheat $(T_w - T_{sat})$ [K]
ΔT_{sub} water subcooling $(T_{sat} - T_p)$ [K]
θ inclination angle [degree].

Subscripts
c center of control volumes bound by the boiling surface
CHF critical heat flux
cu copper
i index along r-coordinate
j index along z-coordinate
min minimum film boiling
o initial at quenching
out from the boiling surface
p water pool
s curved surface
ss asymptotic
Sat saturation
w boiling surface, wall.

Superscripts
$\bar{}$ surface average.

preserve the structural integrity of the reactor vessel [18, 21].

The hemispherical and toroidal geometry of the reactor vessel bottom head provides continually increasing inclination and surface area for vapor generation and flow. Parameters which would influence pool boiling on the outer surface of the vessel bottom head include: surface area, local curvature and inclination, water subcooling, and wall material and thickness. The effects of these parameters need to be understood in order to assess the coolability of an ALWR vessel bottom head by pool boiling. For example, the release of vapor bubbles at lower inclination positions may cause vapor accumulation at higher positions, lowering the pool boiling heat flux. On the other hand, an efficient release of vapor from the edge of the boiling surface can reduce vapor accumulation, and enhance surface coolability. The prevailing scenario, however, will depend upon the geometry and dimensions of the vessel bottom head and the level and subcooling of water in the underlying cavity.

Pool boiling curves are usually based on measurements of the surface average heat flux and wall superheat in experiments that employ either steady-state heating or quenching method. The surface average pool boiling heat fluxes, although useful for assessing overall heat removal rate, may underestimate the local heat flux for a portion of the surface. Therefore, to assess the coolability of an ALWR vessel bottom head, data on both local and average heat fluxes for pool boiling from downward-facing curved surfaces in saturated and subcooled water are needed.

In this work, quenching experiments were performed to investigate the effect of water subcooling on pool boiling from a downward-facing curved surface (radius of curvature, $R_s = 148$ mm) in water. An important question in these experiments was whether the local and surface average maximum and minimum film boiling heat fluxes are representative of quasi steady-state values [22]. For an answer to this question, experiments employed three copper sections of the same diameter (50.8 mm) and surface radius (148 mm), but of different thicknesses (12.8, 20 and 30 mm). Local pool boiling curves obtained at six different locations on the surface (local inclination of 0°–8.26°) were compared with the surface average pool boiling curves for saturation and 5, 10 and 14 K subcooling The effect of surface curvature was assessed by comparing the surface average pool boiling curve for the 12.8 mm thick section with that of Guo and El-Genk [14] for a flat surface section of the same material, diameter and thickness.

EXPERIMENTAL SETUP AND PROCEDURES

Each of the three test sections in the experiments had eight, K-type thermocouples (TC1–TC8) placed ~0.5 mm from the boiling surface and three thermocouples placed near the back surface (TC9–TC11). A cross-sectional view of an instrumented 20 mm thick section is shown in Fig. 1(a). The spacing and the number of these thermocouples were selected to examine the symmetry of pool boiling on the curved surface and to provide sufficient temperature data for subsequent determination of the local and average pool boiling heat fluxes and surface temperatures (see subsection on determination of pool boiling heat flux). The thermocouples were spaced horizontally relative to the centerline as follows: TC1 and TC10 at 0.0 mm, TC2 at 4.25 mm, TC3 and TC7 at 8.5 mm, TC4 at 12.75 mm, TC5, TC8, TC9 and TC11 at 17 mm, and TC6 at 12.25 mm. Thermocouples TC9, TC10 and

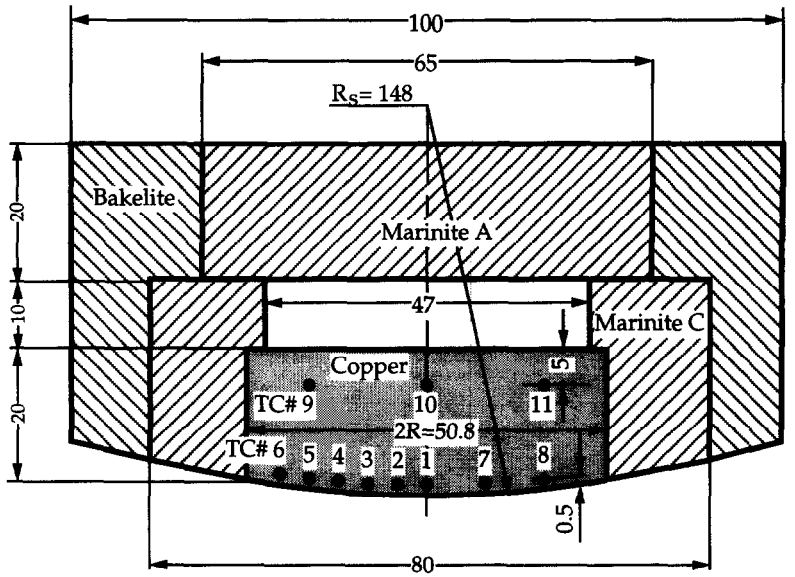

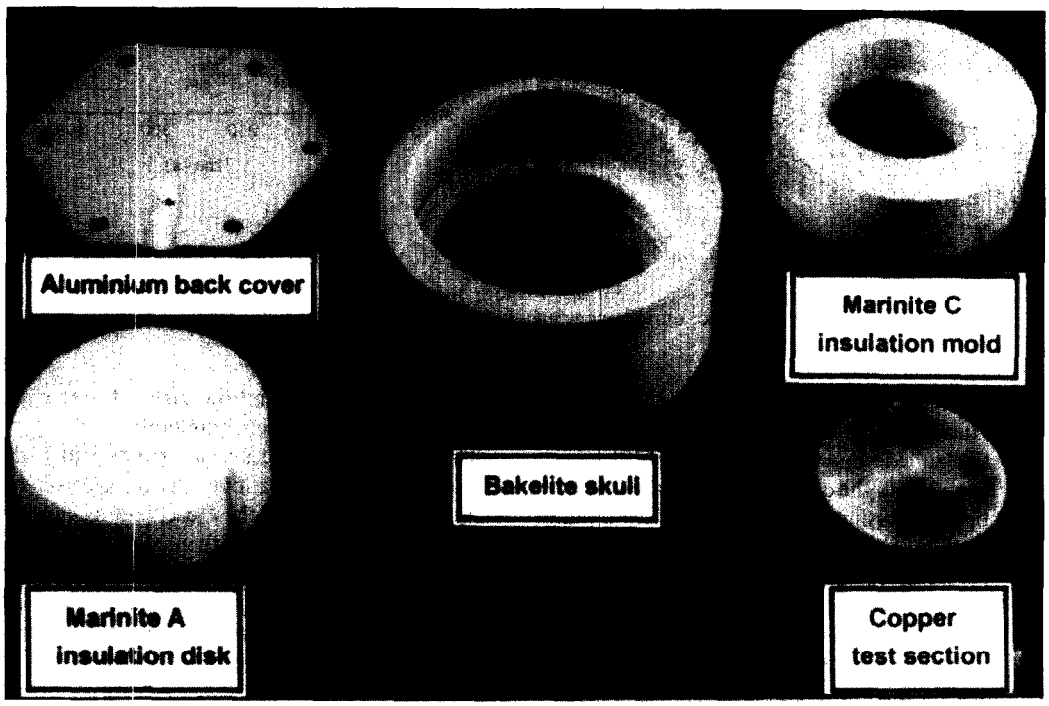

Fig. 1. (a) Cross-sectional view of the 20 mm thick instrumented test section. (b) A photograph of various components of the disassembled test section.

TC11 were placed 4 and 5 mm from the back surface of the 12.8 mm section and of both the 20 and 30 mm sections, respectively. Test sections were thermally insulated on the back and sides using a water sealed mold of Marinite C. A 10 mm space was left between the back surface of the test section and the Marinite C, for routing the leads of the thermocouples to the data acquisition equipment. The test section and the Marinite mold were housed in a cylindrical Bakelite skull for additional insulation and handling. The Marinite mold and the Bakelite skull were machined to the same curvature as the boiling surface in order to avoid edge effects influencing the release of vapor; Figs. 1(a) and 1(b).

The quenching tank, measuring 254 mm × 245 mm × 483 mm (high) in external dimension, is made of aluminum frame with large glass windows on four sides. The windows are for visual observation and recording of pool boiling on the surface using a video camera. To observe the entire boiling surface during quenching, a water sealed mirror was mounted at a 45° angle at the bottom of the tank; Fig. 2(a). The

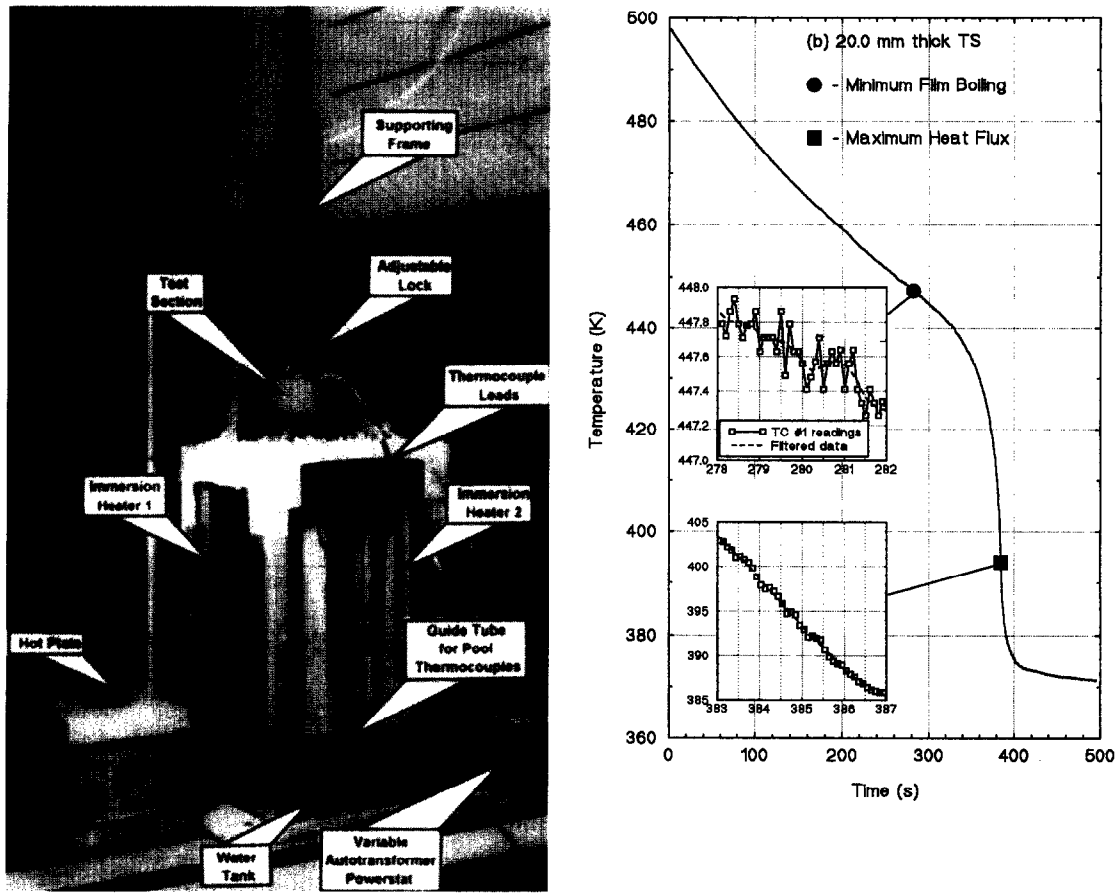

Fig. 2. (a) A photograph of the experiment setup before quenching the test section. (b) Comparison of temperature trace during quenching, before and after numerical filtering.

water in the tank was maintained at the desired temperature during experiments using two, 2.0 kW, individually controlled immersion heaters [13–17].

Prior to each test, the distilled water in the tank was mixed thoroughly using an external circulation pump and degassed by boiling for about 15 min. Also, the curved surface of the copper sections were polished using No. 1200 Silicon Carbide sand paper then cleaned with acetone. To avoid oxidizing the surface before quenching, the test sections were wrapped in aluminum foil while being heated on a hot plate. After being heated to about 510 K, the test sections were lowered into the pool, ~40 mm below the water surface in the quenching tank.

Data recording and processing

During quenching, all eleven thermocouples in the test section were scanned once every 100 ms using a high speed data acquisition unit connected to a 486–50 MHz PC. Because the thermocouples were scanned sequentially, their recording times were adjusted for the time interval (~9 ms) between readings to obtain simultaneous temperature values at the different thermocouple locations. The data was then stored for subsequent processing and analysis. During quenching the boiling process on the surface was recorded using a video camera and the inclined mirror placed at the bottom of the quenching tank.

The raw temperature measurements had high frequency, random oscillations, due to electric equipment. The amplitude of these oscillations varied with the boiling regime during quenching. While in film transition and nucleate boiling, the high-frequency random oscillations had small amplitudes of less than 0.2 K. Near the maximum heat flux, however, the amplitude of these random oscillations was as much as 0.5 K; Fig. 2(b). In order to remove these high frequency, low magnitude random oscillations without unduly degrading the underlying information, numerical filtering (or smoothing) of the raw temperature data was performed using a method similar to that described in [23]. The entire data array was scanned with a window containing a number of data points (three–eleven points) and the data point in the middle of the window was replaced by a value determined from a second degree polynomial fit of the data points in the window. Next, the data point at one end of the window was dropped and the next point at the other end added, and the process was repeated. The width of the smoothing window was adjusted by trial to reduce the high-frequency noise without damping the low frequency desired signal; best results

were obtained using a nine-points window. After numerical filtering, the measured temperatures near the boiling surface were used, in conjunction with the transient heat conduction solution in the test section, to determine the local pool boiling heat fluxes and local temperatures on the boiling surface.

Determination of pool boiling heat flux

The two-dimensional (2D), transient heat conduction in the copper section during quenching can be described by the equation:

$$\rho C_p\left(\frac{\partial T}{\partial t}\right)=\frac{1}{r}\frac{\partial}{\partial r}\left(kr\frac{\partial T}{\partial r}\right)+\frac{\partial}{\partial z}\left(k\frac{\partial T}{\partial z}\right) \quad (1)$$

subject to the following boundary and initial conditions:

$$T(r,z_c,t)=f(r,t)$$

$$k\frac{dT}{dz}(r,0,t)=k\frac{dT}{dr}(R,z,t)=k\frac{dT}{dr}(0,z,t)=0 \quad (2)$$

$$T(r,z,0)=T_o.$$

where,

$$z_c=(H-0.005)+\sqrt{R_c^2-r^2}-\sqrt{R_c^2-R^2} \quad (3a)$$

$$R_c=(R^2+\delta^2)/2\delta \quad (3b)$$

and,

$$\delta=(R_s-\sqrt{R_s^2-R^2})(H-0.005)/H. \quad (4)$$

During quenching, the back and sides of the copper section are assumed adiabatic (equation (2)). The symmetry of heat transfer from the boiling surface (equation (2)), confirmed by the temperature measurements made near the boiling surface (TC1–TC8) [17], justified the use of a 2D (r,z) transient heat conduction analysis of the test section during quenching; Figs. 3(a) and 3(b). Figure 3(b) shows the curve fitted temperature measurements by TC1–TC8 at different times during quenching of the 20 mm thick section. In the analysis, the physical properties (k, C_p and ρ) of copper were taken to be temperature dependent. Since temperatures in the copper section were measured near the boiling surface (TC1–TC8), it was easier to use direct transient conduction (equation (1)), rather than inverse conduction, to determine the local pool boiling heat fluxes and surface temperatures during quenching. Equation (1) was solved numerically using the recorded temperatures near the boiling surface (TC1–TC8), as a boundary condition, equation (5) and Fig. 3(b), to derive the local surface heat fluxes and temperatures as functions of time during quenching [17]. The temperature boundary condition near the boiling surface (Fig. 3(a) and equation (2)) is given as:

$$f(r,t)=a_0+a_1\cos(\pi(r/R)^{a_2}). \quad (5)$$

Equation (5) is a polynomial fit of measured temperatures near the boiling surface as a function of time during quenching; Fig. 3(b). The coefficients a_0, a_1 and a_2 were determined from the least square fit of the temperature measurements (TC1–TC8) recorded at the same instant in time during quenching.

Numerical solution

The numerical solution of equation (1) employed a fully implicit alternating direction, finite control volume (CV) method [24] to ensure stability of the solution and reduce the storage and computational time on a 486–50 MHz PC. The solution used a (20×20) grid to represent the calculation domain within the test section, Fig. 3(a), and a convergence coefficient of 10^{-6}. The orthogonality of the heat flux with respect to the surfaces of CVs in the calculation grid was handled by calculating the temperature gradient from the derivative along the unit vector normal to the surface. The temperature derivatives were based on linear interpolation of temperatures along the lines passing through the centers of CVs. When a (30×30) grid and/or a smaller convergence coefficient were used, computation time increased significantly with negligible changes in the calculated heat flux and surface temperature values.

The temperatures within the copper section were calculated at the center and the heat fluxes determined at the boundaries of the control volumes. The local heat flow at the boiling surface was determined from the heat balance in the control volumes (CVs) bounded by the boiling surface; Fig. 3(a). The local pool boiling heat flux was then determined by dividing the calculated heat flow by the corresponding surface area of the control volume. The corresponding local surface temperatures were determined from the parabolic extrapolation of the calculated temperatures at centers of CVs in the three rows near the boiling surface. The surface average pool boiling heat flux was determined by dividing the calculated total heat flow from the boiling surface by its total surface area. The corresponding average wall temperature was determined from the integral of the local wall temperatures over the entire boiling surface.

The accuracy of the numerical calculations was confirmed by performing an overall energy balance after each time interval; calculations were accurate to within less than 1.0%, and by comparing calculated and measured temperatures by TC9–TC11; the difference was of the same order of magnitude as the uncertainty in the thermocouples measurements, about ±0.5. Determined from sensitivity analyses performed using the 2D numerical solution of transient conduction in the copper section, the uncertainty in calculated pool boiling heat flux was about $\pm1.4\%$ due to the uncertainty in the location of TCs near the boiling surface, $\pm1.7\%$ due to the uncertainty in TC readings, $\pm3.4\%$ due to numerical filtering of raw temperature data, and $\pm1.7\%$ due to curve fitting of measured temperatures near the boiling surface. Based on these values, the overall uncertainty, determined using the method outlined in [25], in the

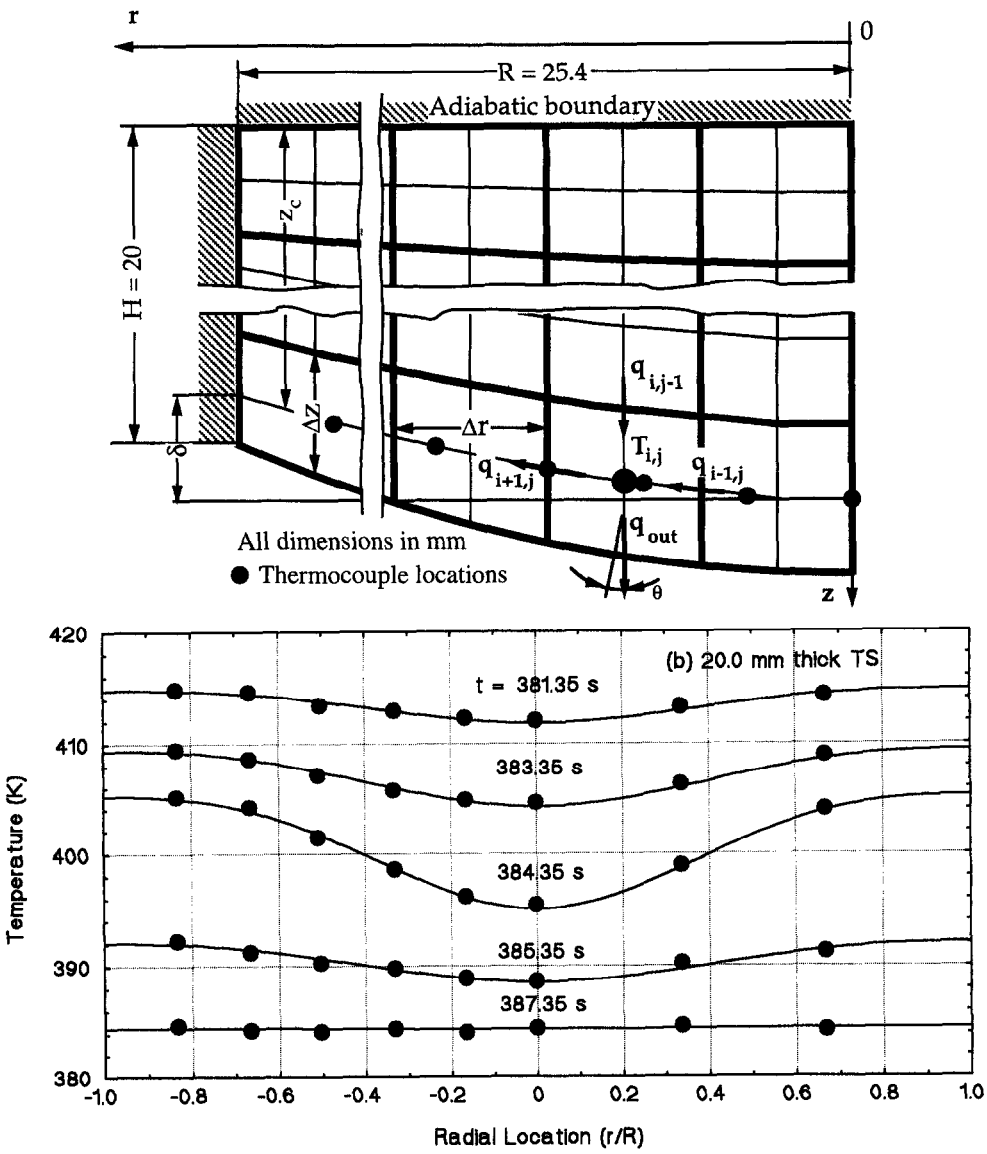

Fig. 3. (a) Calculation grid for the 2D transient heat conduction numerical model. (b) Curve fitting of temperatures measured in copper section near boiling surface.

maximum and the minimum film boiling heat fluxes was $\pm 4.5\%$ and $\pm 9\%$, respectively. The uncertainty in the surface average maximum and minimum film boiling heat fluxes was $\pm 2\%$ and $\pm 4\%$, respectively.

RESULTS AND DISCUSSION

Experimental results presented in the following subsections show the effects of water subcooling on both the local and surface average pool boiling curves and identify the proper test section thicknesses for which the boiling curves are representative of quasi steady-state. The results also delineate the effect of local inclination on local pool boiling heat flux and wall superheat. In order to quantify the effect of surface curvature on pool boiling, the surface average saturation pool boiling curve for the 12.8 mm thick section was compared with that of Guo and El-Genk [13] for a flat surface section of identical diameter, material and thickness. The local pool boiling curves presented are the average of two separate tests performed at the same conditions to confirm the reproducibility of experimental results [17]. Local pool boiling curves were reproducible to within less than $\pm 5\%$.

Visual observations and video images of the boiling surface during quenching revealed that the destabilization and collapse of the film boiling in saturation experiments were hydrodynamic in nature, Figs. 4(a) and (b), but thermally driven in subcooled boiling. In saturation film boiling, all the heat released from the surface is consumed in vapor generation. The flow of vapor under the effect of the tangential gravity component causes the film thickness to be smallest at the lowermost position and largest near the edge of the

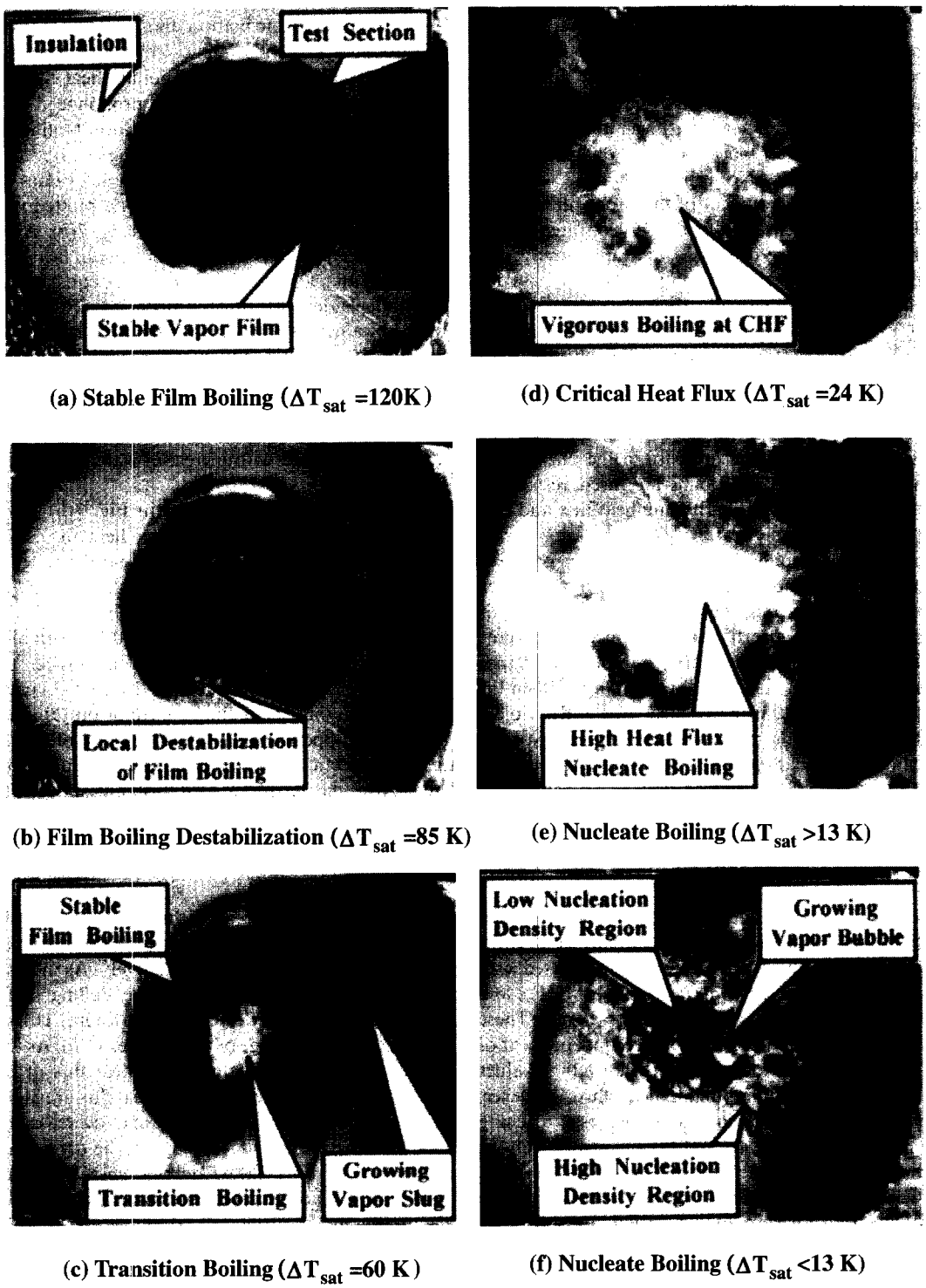

Fig. 4. Photographs of boiling surface of 20 mm thick section during quenching in saturated water.

boiling surface. At high wall superheat, intermittent releases of vapor slugs from the periphery of the swelled vapor film caused the vapor–liquid interface to oscillate repetitively, then fully stabilize as excess vapor in the film was released; Fig. 4(b). As the surface temperature decreased with time in film boiling, the average size of the vapor slugs and their frequency of release decreased. Eventually, induced film oscillations, following the release of vapor slugs, destabilized film boiling, marking the minimum film boiling heat flux and the beginning of transition boiling.

In subcooling film boiling, however, only a fraction

of the heat released from the curved surface is consumed in vapor generation; the largest fraction is conducted through the vapor film to the underlying water pool, where it is removed by natural convection. Initially, vapor generated at the lower positions on the surface accumulates and increases the film thickness at higher locations. No vapor, however, was seen released from the periphery of the vapor film, apparently due to condensation by subcooled water. As the surface temperature dropped, less vapor was generated, and the film thickness continued to decrease due to condensation. Eventually, the vapor film collapsed as the surface temperature approached that corresponding to the minimum film boiling heat flux. The duration of film boiling in saturation boiling (~ 384 s) was much shorter than in subcooled boiling experiments (713, 540 and 448 s for ΔT_{sub} of 5, 10 and 14 K, respectively). The decrease in the duration of film boiling as water subcooling increased, resulted in both higher minimum film boiling heat flux and corresponding wall superheat.

In transition boiling, intense nucleation occurred initially in the middle portion of the surface, then propagated outward as the wall superheat decreased; Fig. 4(c). The outer portion of the surface was covered with a relatively thick vapor film and the excess vapor was released from the edge as vapor slugs. When the maximum heat flux was reached, Fig. 4(d), violent and energetic vapor generation and release, involving the entire surface, occurred. In all experiments, the maximum heat flux occurred first at the lowermost position then sequentially at the higher inclination positions.

Effect of wall thickness

Figure 5 shows that in saturation and subcooled pool boiling experiments, local and surface average maximum heat fluxes increased with increased wall thickness reaching asymptotic values, MHF_{ss} and $\overline{MHF}_{ss}$, respectively, at wall thickness > 19 mm. These values of the maximum heat flux were independent of wall thickness. The local and surface average values of the minimum film boiling heat flux, however, decreased with increased wall thickness, reaching asymptotic values, $(q_{min})_{ss}$ and $(\overline{q_{min}})_{ss}$, respectively, at approximately the same wall thickness of 19 mm (Fig. 6). The effect of test section thickness on the maximum heat flux is similar to that reported previously by Westwater *et al.* [22] and Peyayopanakul and Westwater [26] in a series of quenching tests of copper blocks with liquid nitrogen on the face-up, horizontal flat surface. Their results showed that for test sections $\geqslant 25$ mm in thickness, maximum heat flux was independent of wall thickness and the pool boiling curves were all quasi-steady state and equivalent to those obtained in steady-state heating tests [26]. This wall thickness is about 31% higher than that indicated by the present data in Figs. 5 and 6. In saturation boiling, Figs. 5 and 6 show both the maximum and the minimum film boiling heat fluxes to increase with decreased surface inclination and/or increased water subcooling. The dependence of both the local maximum and minimum film boiling heat fluxes on wall thickness < 19 mm is more pronounced at the lower inclination positions in saturation boiling, and at all inclinations in subcooled boiling.

The surface average maximum heat flux values were divided by their asymptotic values and plotted vs the corresponding Biot number, *Bi*, in Fig. 7(a). As this figure indicates, the normalized maximum heat fluxes for the 20 and 30 mm thick sections are equal to unity and independent of Biot number $\geqslant 0.8$. This Biot number value is slightly lower than that reported by Westwater *et al.* [22] for saturation pool boiling from upward facing surfaces of different metals ($Bi = 0.9$). For the 12.8 mm thick section, however, $Bi < 0.8$ and the normalized maximum heat fluxes are less than unity and decrease with increased water subcooling; Fig. 7(a).

Similar results are delineated in Fig. 7(b) for the normalized minimum film boiling heat fluxes. The normalized minimum film boiling heat fluxes for the 20 and 30 mm thick sections are equal to unity and independent of Biot number $\geqslant 0.008$. For the 12.8 mm thick section, however, $Bi < 0.008$ and the normalized minimum film boiling heat fluxes are higher than unity. The results presented in Figs. 5–7, clearly demonstrate that the boiling curves of the 20 and 30 mm thick copper sections, and not those of the 12.8 mm thick section, are representative of quasi steady-state. Also, the maximum heat flux values for the two thicker sections are representative of the quasi steady-state critical heat flux [22, 26].

Pool boiling curves

Figures 8(a)–(d) present the local pool boiling curves of the 20 mm thick section for saturation and 5, 10 and 14 K subcooling, respectively. As indicated earlier, the local inclination on the boiling surface varied from $\theta = 0°$ (lowermost position, TC1) to $\theta = 8.26°$ (near the edge of the surface, TC6). As these figures show, the nucleate boiling heat flux at high wall superheat and the maximum heat flux are highest at $\theta = 0°$ (lowermost position) and decrease as θ increases. Also, nucleate boiling can be divided into two distinct regions: (a) *a high wall superheat nucleate boiling*, where heat flux increases with decreased local inclination on the surface and (b) *a low wall superheat nucleate boiling*, where the heat flux increases with increased local inclination. Figure 8(a) shows that the transition from the high to the low wall superheat nucleate boiling occurs at $\Delta T_{sat} \sim 13$ K in saturation pool boiling and increases with water subcooling to 15 and 15.5 K at 5 K and both 10 and 14 K subcooling, respectively. The dependence of the nucleate boiling heat flux on surface inclination shown in Figs. 8(a)–(d) is opposite to that reported earlier for inclined flat surfaces by Beduz *et al.* [2] and Nishikawa *et al.* [9] in their steady-state heating experiments and by Guo and El-Genk in their quenching experiments [15, 16].

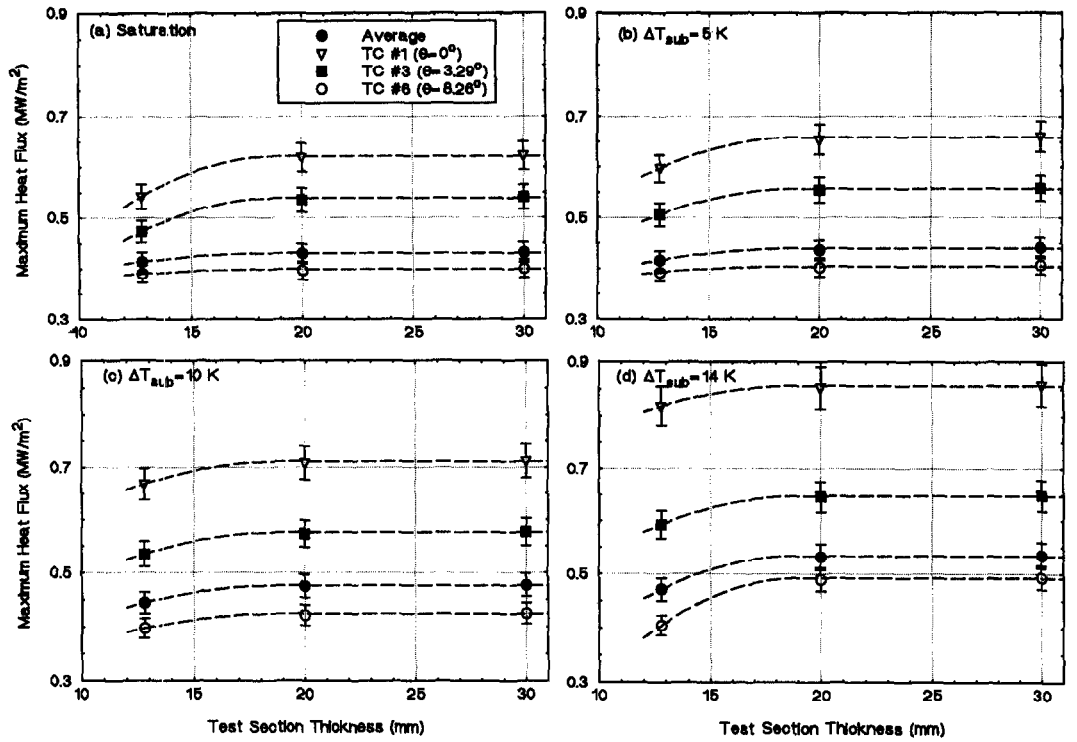

Fig. 5. Effect of test section thickness and subcooling on the maximum pool boiling heat flux.

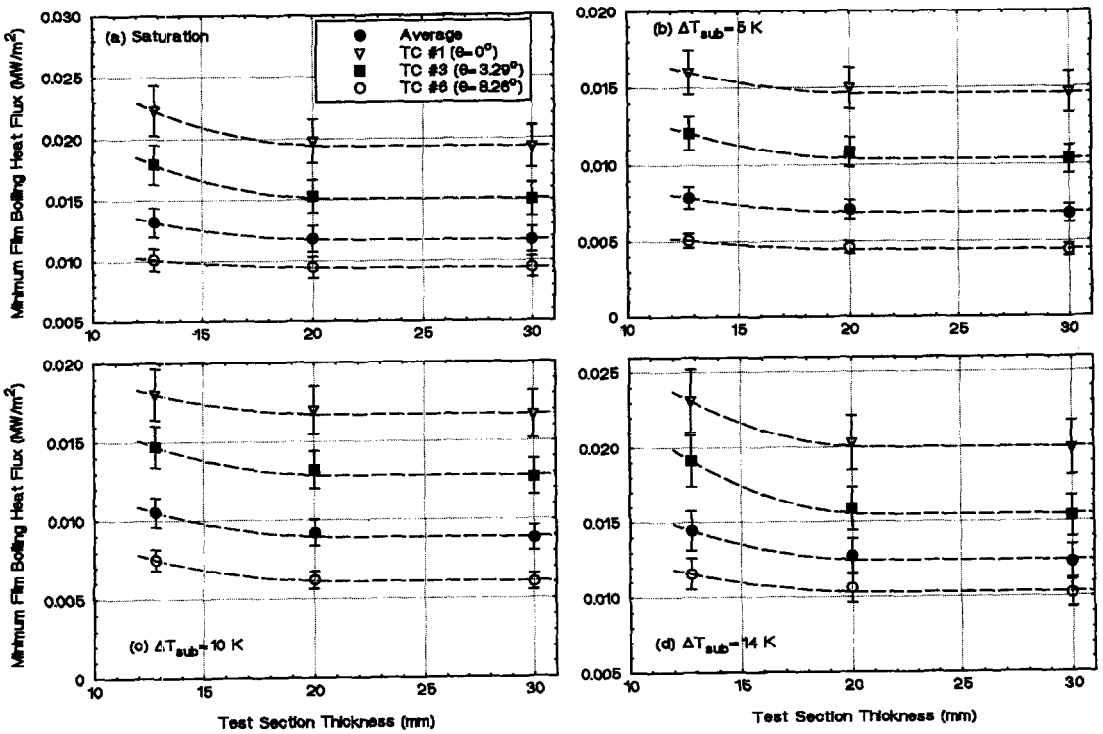

Fig. 6. Effect of test section thickness and subcooling on the minimum film boiling heat flux.

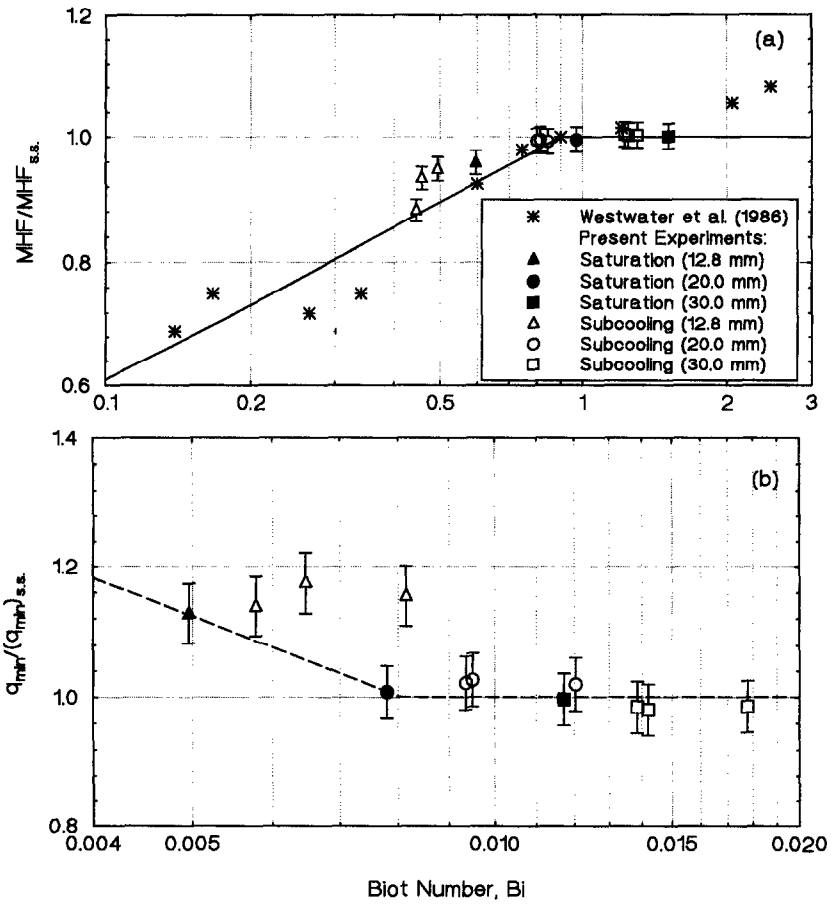

Fig. 7. (a) Biot number values corresponding to surface average maximum heat fluxes. (b) Biot number values corresponding to surface average minimum film boiling heat fluxes.

The enhanced nucleate boiling at the low inclination positions on the curved surfaces at high wall superheat is caused by high nucleation density and efficient bubble release; Fig. 4(e). The visual observations and video images of the boiling surface in the experiments showed intense bubble nucleation and growth occurring in the middle portion of the surface, accompanied by vapor release in a pulsating radial motion, as was recently reported in large scale tests [18]. The lower nucleate boiling heat fluxes at the higher inclination positions, however, are caused by the accumulation of the vapor generated at the lower positions on the surface. In nucleate boiling at low wall superheat, however, the rate and density of bubble nucleation in the middle portion of the surface decreased, but intensified in the outer portion of the surface; Fig. 4(f). Consequently, the nucleate boiling heat flux at higher locations on the surface was higher than at lower inclination positions. Because vapor bubbles were released readily from the edge of the boiling surface, little vapor accumulated on the surface at higher locations.

In transition and film boiling, the dependence of the heat flux on θ is opposite to that in nucleate boiling at low wall superheat, but the same as for the maximum heat flux and in nucleate boiling at high wall superheat. Also, the transition from film to transition boiling appears to be somewhat sharper at the lowermost position ($\theta = 0°$) than at the higher inclination positions on the surface and in subcooled boiling.

Effect of water subcooling

Figures 5 and 6 show that in subcooled boiling, both the local maximum and minimum film boiling heat fluxes increase with decreased surface inclination and/or increased subcooling. Figure 9 also shows the effect of water subcooling on local pool boiling curves at different locations on the surface and on the surface average pool boiling curves for the 20 mm section. In all boiling regimes, the heat flux increases as water subcooling increases. However, at saturation, the minimum film boiling heat flux and the corresponding wall superheat are significantly higher than those in subcooled boiling, because the quenching mechanisms of film boiling in saturation and subcooled boiling experiments were different. As indicated earlier, the destabilization and collapse of the vapor film in satu-

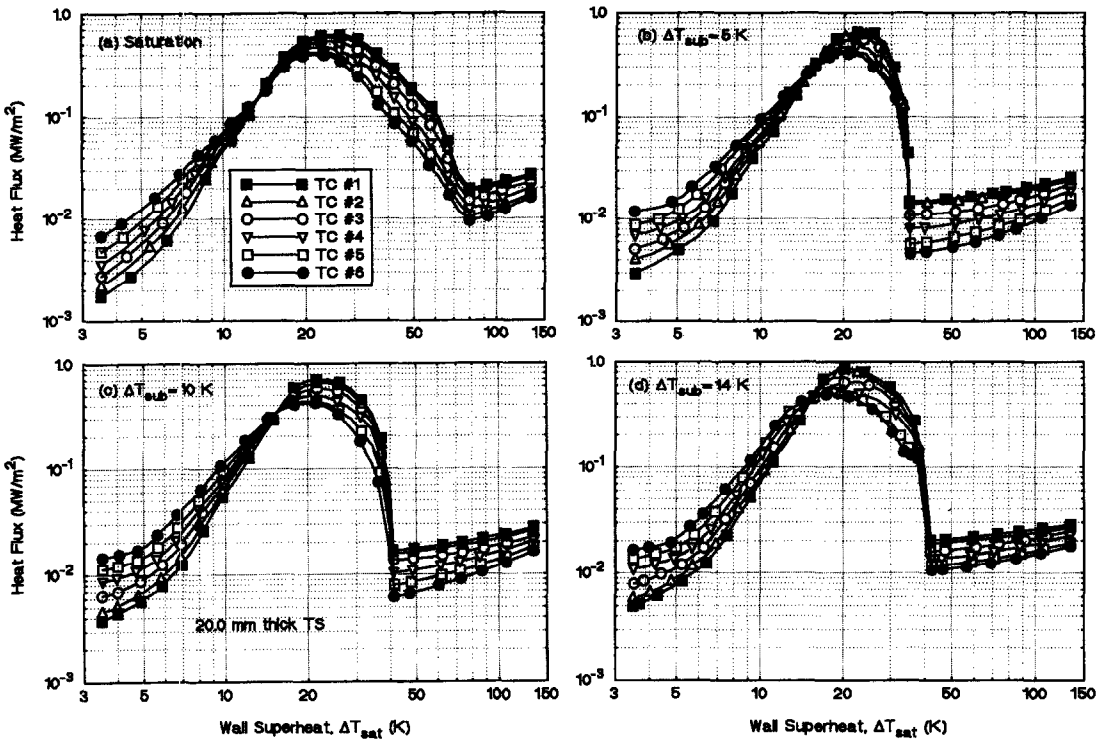

Fig. 8. Effect of water subcooling on the local pool boiling curves for the 20 mm thick section.

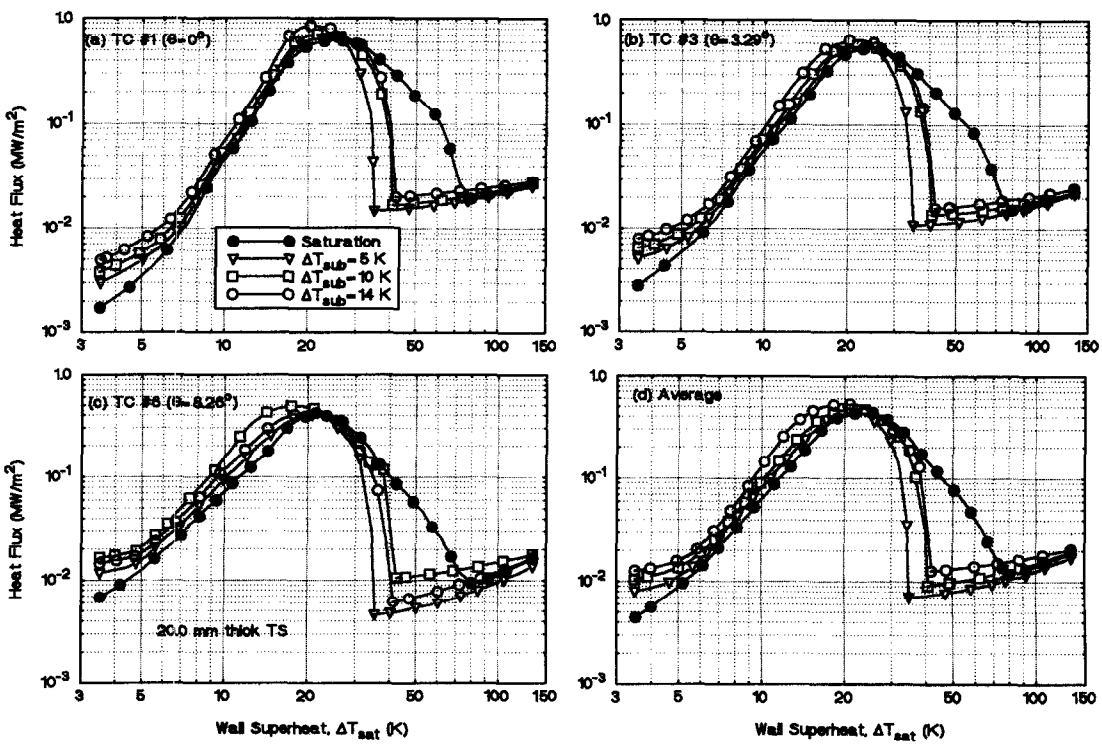

Fig. 9. Effect of water subcooling on the local and surface average pool boiling curves for the 20 mm thick section.

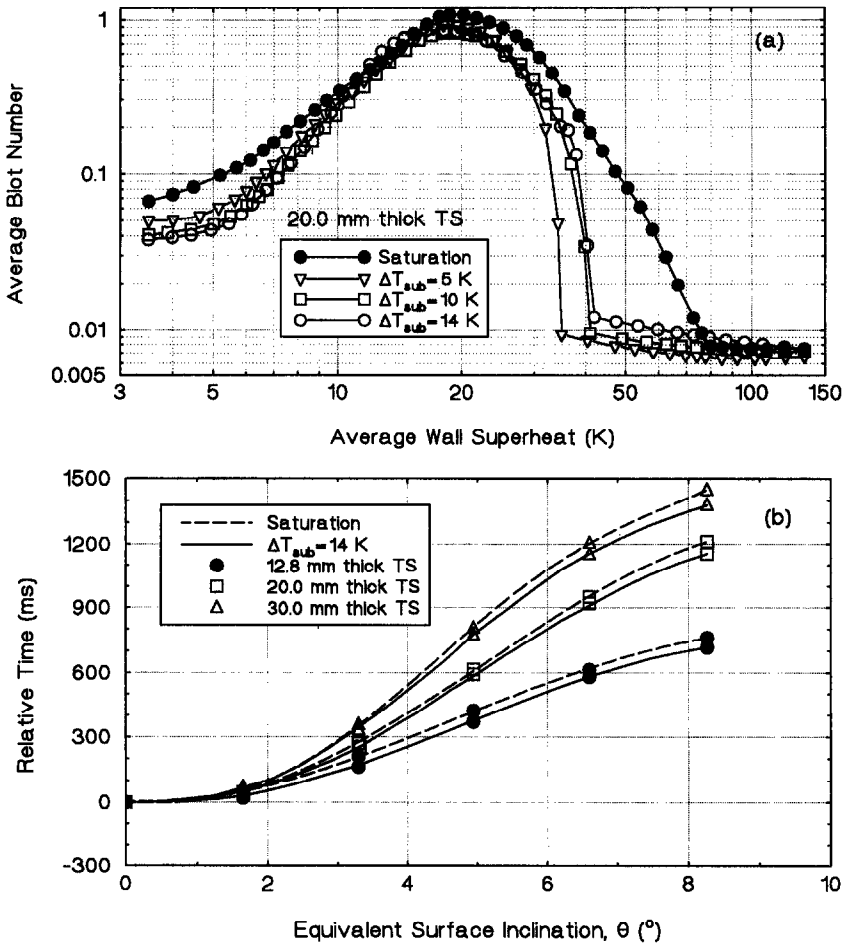

Fig. 10. (a) Effect of water subcooling on the surface average Biot number. (b) Effect of water subcooling and wall thickness on relative quenching time.

ration boiling was hydrodynamic in nature, but thermally driven in subcooling boiling.

The results presented in Fig. 10(a) delineate the effect of water subcooling on the surface average Biot number. In film boiling and in the lower portion of transition boiling ($\Delta T_{sat} > 33$–48 K), Biot number is less than 0.1, suggesting that in subcooled boiling the heat released from the surface was easily removed by evaporation and convection in the liquid. In the upper portion of both transition boiling ($\Delta T_{sat} < 33$ K) and in nucleate boiling at $\Delta T_{sat} > 5.2$–7.2 K, Biot number values are higher than 0.1, indicating the effectiveness of heat removal from the surface by boiling. Figure 10(a) also shows Biot number corresponding to the maximum heat flux to be in excess of 1.0 for saturation pool boiling and decreases with increased water subcooling.

Quenching time

Results show that the thickness of the test section does not affect the order of occurrence of the maximum heat flux at the different locations on the surface during quenching, but rather its value and the time when it occurs; Fig. 10(b). For example, the maximum heat flux for the 12.8 mm thick section occurs at the lowestmost position after 215 s compared to 384 s (79% longer) for the 20 mm thick section. For all three sections, the maximum heat flux occurs first at the lowermost position then at the higher locations in an orderly sequence. The difference in time between subsequent maximum heat flux occurrences increases as the thickness of the test section increases and/or water subcooling decreases.

In Fig. 10(b), the time during quenching is normalized to that corresponding to the occurrence of maximum heat flux at the lowermost position to compare subsequent events occurring at higher locations on the surface. At TC6 location, it took the 20 mm thick section 72% more time than the 12.8 mm thick section to reach the maximum heat flux. The high energy storage in the 20 mm thick section resulted in a larger accumulation of vapor on the surface, causing the progression of the maximum heat flux events on the surface to be relatively slower than for the 12.8

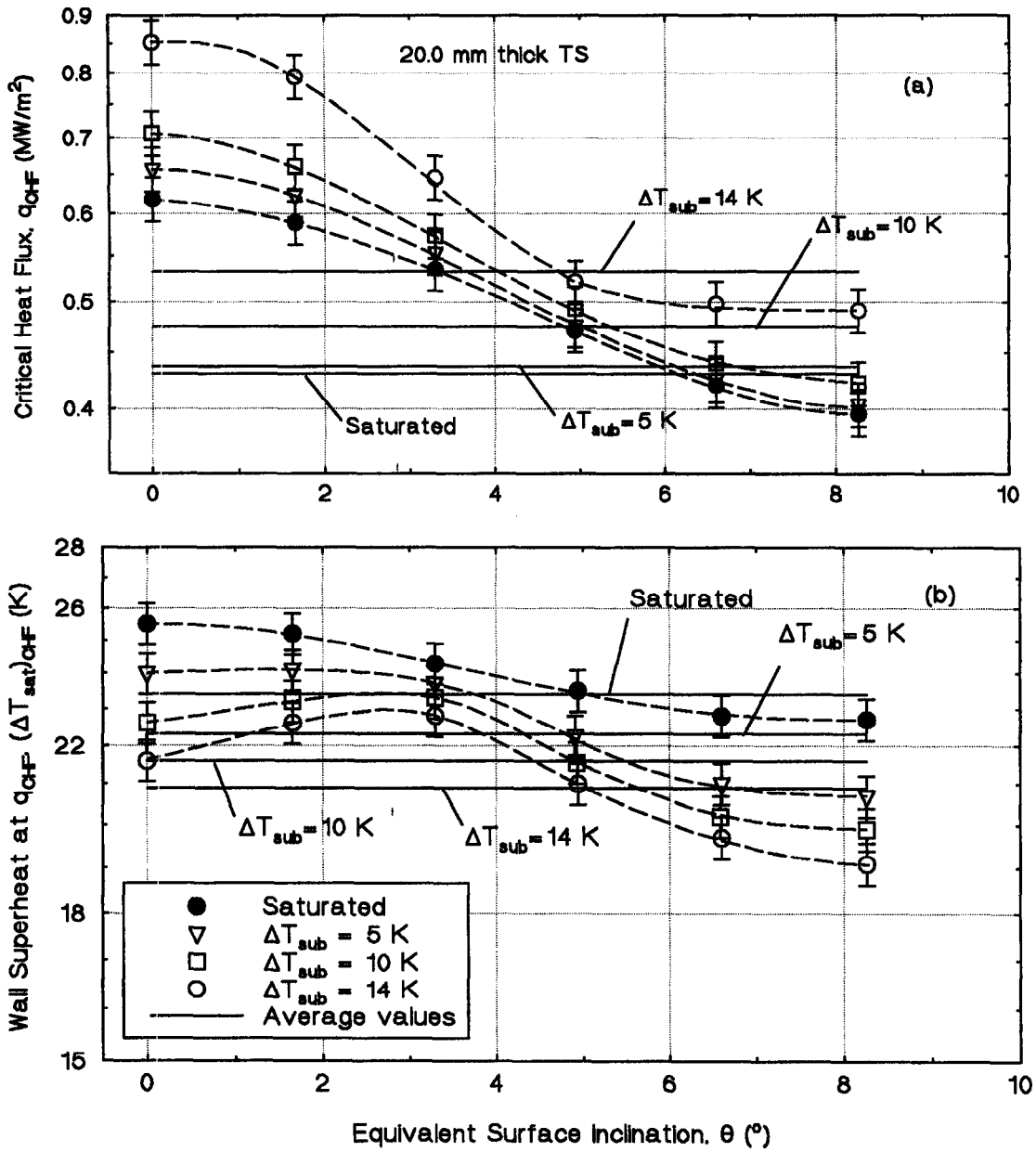

Fig. 11. Comparison of local and surface average maximum pool boiling heat fluxes and the corresponding wall superheats for the 20 mm thick section.

mm thick section. Figure 10(b) also shows that the relative quenching time decreases slightly with increased water subcooling.

Maximum heat flux

The local and surface average values of the maximum heat flux and the corresponding wall superheats, for saturation and subcooled boiling are presented in Figs. 11(a) and (b), respectively. Figure 11(a) shows the maximum heat flux decreases with increased local inclination, but increases with increased water subcooling. The wall superheat corresponding to either the local or the average maximum heat flux generally decreases with increased surface inclination and/or increased subcooling. Also, for a given pool temperature, the lower inclination positions on the surface are more coolable than indicated by MHF. At higher inclination positions, however, MHF overestimates surface coolability, whereas the extent of the high and low coolability portions of the surface strongly depend on water subcooling. For example, the saturation MHF underestimates the coolability of the surface portion with $\theta \leqslant 6°$, but overestimate the coolability of the outer surface portion with higher inclination. At 14 K water subcooling, the extent of the inner portion of the surface with

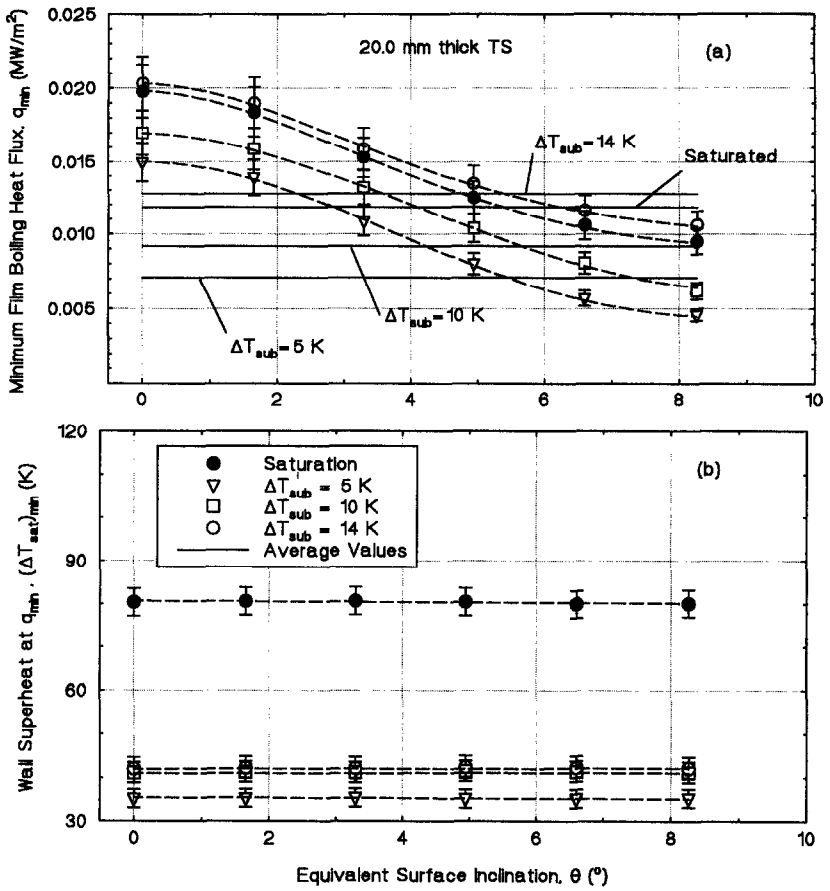

Fig. 12. Comparison of local and surface average minimum film boiling heat fluxes and the corresponding wall superheats for the 20 mm thick section.

MHF > $\overline{\text{MHF}}$ extends only to $\theta < 5°$. Therefore, care should be taken when using $\overline{\text{MHF}}$ to assess the coolability of the entire curved surface.

Minimum film boiling heat flux

Figures 12(a) and (b) compare the local and the surface average minimum film boiling heat fluxes and the corresponding wall superheats at different water subcooling. The minimum film boiling heat flux decreases with increased inclination and/or decreased subcooling. At saturation, however, the minimum film boiling heat flux is significantly higher than that at 5 K subcooling, and only slightly lower than that for 14 K subcooling. As indicated earlier, because film boiling destabilization in saturation boiling is hydrodynamically driven, minimum film boiling occurs at higher heat flux and wall superheat. Although independent of surface inclination, the corresponding wall superheats increases with increased water subcooling; Fig. 12(b).

Effect of surface curvature

As indicated earlier, the local and surface average pool boiling curves of the 12.8 mm thick section are not representative of the quasi steady-state phenomena. Therefore, the boiling curves for this section include both the transient and surface curvature effects. Nevertheless, a comparison of the surface average pool boiling curve for this section with that of a flat surface section of the same dimensions and material [13], would quantify the effect of surface curvature on pool boiling (Fig. 13). As this figure indicates, pool boiling heat fluxes for the curved surface section are significantly higher in film boiling, transition boiling and nucleate boiling at high wall superheat. The $\overline{\text{MHF}}$ for the curved surface (0.41 MW m^{-2}) is almost twice that of the flat surface (0.21 MW m^{-2}) and $\overline{q_{min}}$ (13 kW m^{-2}) is more than six times that for the flat surface (2 kW m^{-2}).

Also, the wall superheat corresponding to $\overline{\text{MHF}}$ (23.5 K) and $\overline{q_{min}}$ (90 K) is 11.5 and 60 K higher than those for the flat surface, respectively. In nucleate boiling at low wall superheat, however, the heat fluxes for the flat surface section are higher than those for the curved surface, at the same wall superheat. The high nucleate boiling heat flux for the flat surface section could be caused by the mixing induced in the boundary layer by the vapor bubbles as they detached and slid on the surface toward the edge of the test section, where they were released [13].

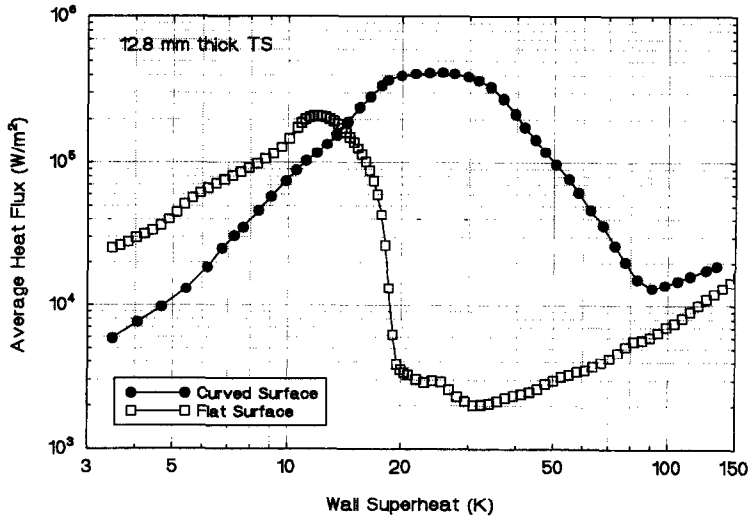

Fig. 13. Effect of the surface curvature on the surface average pool boiling curves for the 12.8 mm thick section.

SUMMARY AND CONCLUSIONS

Quenching experiments were performed to investigate pool boiling from downward-facing curved surfaces in water at saturation and 5, 10 and 14 K subcooling. Experiments, employed three copper sections of the same diameter (50.8 mm) and surface radius (148 mm), but of different thicknesses (12.8, 20 and 30 mm). The pool boiling data of the 20 and 30 mm thick sections, but not that of the 12.8 mm thick section, was representative of quasi steady-state and the maximum heat flux values were representative of the quasi steady-state critical heat flux. Nucleate boiling can be divided into two distinct regions: *high wall superheat*, where heat flux decreases with increased local inclination, and *a low wall superheat*, where heat flux increases with increased inclination. This dependence of nucleate boiling heat flux on local surface inclination is opposite to that reported earlier by other investigators for flat, inclined surfaces.

The local and average maximum heat fluxes increased, but the corresponding wall superheat decreased, with increased water subcooling. The local minimum film boiling heat flux also decreased with increased surface inclination, however, the corresponding wall superheat was independent of surface inclination, but increased with increased subcooling. The values of the minimum film boiling heat flux and the corresponding wall superheat for saturation boiling, were higher than those for subcooled boiling at $\Delta T_{sub} \leqslant 14$ K, because the quenching of film boiling in the former was hydrodynamically driven while that in the latter was thermally driven.

The surface average heat fluxes of the 12.8 mm thick section in film and transition boiling, and in nucleate boiling at high wall superheat were significantly higher than those for a flat surface section of the same dimensions and material. The value of $\overline{MHF}$ for the curved surface section (0.41 MW m^{-2}) was almost twice that of the flat surface section and $\overline{q_{min}}$ (13 kW m^{-2}) was more than six times that for the flat surface section. Also, the wall superheat corresponding to $\overline{MHF}$ and $\overline{q_{min}}$ was 11.5 K and 60 K higher than those for the flat surface section, respectively. In nucleate boiling at low wall superheat, however, the pool boiling heat fluxes for the flat surface section were higher than those for the curved surface section.

Acknowledgements—This research is sponsored by the University of New Mexico's Institute for Space and Nuclear Power Studies.

REFERENCES

1. R. P. Anderson and L. Bova, The role of down facing burnout in post-accident heat removal, *Trans. Am. Nucl Soc.* **14**, 294–304 (1971).
2. C. Beduz, R. G. Scurlock and A. J. Sousa, Angular dependence of boiling heat transfer mechanisms in liquid nitrogen, *Adv. Cryogenic Engng* **33**, 363–370 (1988).
3. L. T. Chen, Heat transfer to pool boiling freon from inclined heating plate, *Lett. Heat Mass Transfer* **5**, 111–120 (1978).
4. P. M. Githinji and R. H. Sabersky, Some effects on the orientation of the heating surface in nucleate boiling, *J. Heat Transfer* **85**, 379 (1963).
5. S. Ishigai, K. Inoue, Z. Kiwaki and T. Inai, Boiling heat transfer from a flat surface facing downward, *Proceedings International Heat Transfer Conference*. Paper No. 26 (1961).
6. D. S. Jung, J. E. S. Venart and A. C. M. Sousa, Effects of enhanced surfaces and surface orientation on nucleate and film boiling heat transfer in R-11, *Int. J. Heat Mass Transfer* **30**(12), 2627–2639 (1987).
7. D. N. Lyon, Boiling heat transfer and peak nucleate boiling fluxes in saturated liquid helium between the λ and critical temperatures, *Adv. Cryogenic Engng* **19**, 371–378 (1964).
8. B. D. Marcus and D. Dropkin, The effect of surface configuration on nucleate boiling heat transfer, *Int. J. Heat Mass Transfer* **6**, 863–867 (1963).
9. K. Nishikawa, Y. Fujita, S. Uchida and H. Ohta, Effect of heating surface orientation on nucleate boiling heat

transfer, *Proceedings of the ASME–JSME Thermal Engineering Joint Conference*, Vol. 1, pp. 129–136 (1983).
10. S. Nishio and G. R. Chandratilleke, Steady-state pool boiling heat transfer to saturated liquid helium at atmospheric pressure, *JSME Int. J. Series I*, **32**(4), 639–945 (1989).
11. N. Seki, S. Fukushako and K. Torikoshi, Experimental study on the effect of orientation of heating circular plate on film boiling heat transfer for fluorocarbon refrigerant R-11, *J. Heat Transfer* **100**, 624–628 (1978).
12. I. P. Vishnev, I. A. Filatov, Ya. G. Vinokur, V. V. Gorokhov and G. G. Svalov, Study of heat transfer in boiling of helium on surfaces with various orientations, *Heat Transfer–Sov. Res.* **8**(4), 104–108 (1976).
13. Z. Guo and M. S. El-Genk, An experimental study of saturated pool boiling from downward facing and inclined surfaces, *Int. J. Heat Mass Transfer* **35**(9), 2109–2117 (1992).
14. Z. Guo and M. S. El-Genk, Effects of liquid subcooling on the quenching of inclined and downward-facing flat surfaces in water, *AIChE Symp. Ser.* No. 288, **88**, 241–148 (1992).
15. M. S. El-Genk and Z. Guo, Saturated and subcooled pool boiling from downward-facing and inclined surfaces. In *Flow and External Flow Boiling* (Edited by V. K. Dhir and A. E. Bergles), pp. 243–249. ASME, New York (1992).
16. M. S. El-Genk and Z. Guo, Transient boiling from inclined and downward-facing surfaces in a saturated pool, *Int. J. Refrig.* **16**(6), 414–422 (1993).
17. M. S. El-Genk, A. G. Glebov and Z. Guo, Pool boiling from downward-facing curved surface in saturated water, *Proceedings of the Tenth International Heat Transfer Conference*, Vol. 5, pp. 45–50. Brighton, England 14–18 August (1994).
18. T. Y. Chu, B. L. Bainbridge, J. H. Bents and R. B. Simpson, Observation of quenching of downward-facing surfaces, SANDIA Report, SAND93-0688 · UC-940, Sandia National Laboratories, Albuquerque, NM (January 1994).
19. J. O'Brien and G. Hawkes, Thermal analysis of a reactor lower head with core relocation and external boiling heat transfer, *AIChE Symp. Ser.* No.283, **87**, 159–168 (1991).
20. H. Park and V. K. Dhir, Steady-state thermal analysis of external cooling of a PWR vessel lower head, *AIChE Symp. Ser.* No. 283, **87**, 1–7 (1991).
21. R. E. Henry, J. P. Burelbach, R. J. Hammersley, C. E. Henry and G. T. Klopp, Cooling of core debris within the reactor vessel lower head, *J. Nucl. Technol.* **101**, 385–399 (1993).
22. J. W. Westwater, J. J. Hwalek and M. E. Irving, Suggested standard method for obtaining boiling curves by quenching, *J. Ind. Engng Fundam.* **25**, 685–692 (1986).
23. A. Savitzky and M. J. E. Golay, Smoothing and differentiation of data by simplified least square procedures, *Anal. Chem.* **36**, 1627–1639 (1964).
24. S. V. Patankar, *Numerical Heat Transfer and Fluid Flow*. Hemisphere, Washington, D.C. (1980).
25. M. Kline and F. A. McClintock, Describing uncertainties in single-sample experiments, *Mech. Engng*, 3–8 January (1953).
26. W. Peyayopanakul and J. W. Westwater, Evaluation of the unsteady-state quenching method for determining boiling curves, *Int. J. Heat and Mass Transfer* **21**, 1437–1445 (1978).